Comparison of Two Algorithms for Signal Detection in Pulsar-based FSR

H. Kabakchiev[1], V. Behar [2], I. Garvanov[3], D. Kabakchieva[4], A. Kabakchiev[5], H. Rohling[6], M. Bentum[7], J. Fernandes[8]

[1] Sofia University "St. Kliment Ohridski"
Sofia, BULGARIA
email: ckabakchiev@fmi.uni-sofia.bg

[2] Institute of Information & Communication Technologies
Sofia, BULGARIA
email: behar@bas.bg

[3] University of Library Studies & Information Technologies
Sofia, BULGARIA
email: i.garvanov@unibit.bg

[4] University of National and World Economy
Sofia, BULGARIA
email: d.kabakchieva@unwe.bg

[5] Air Traffic Service Authority – "BULATSA" Technologies
Sofia, BULGARIA
email: av.kab@abv.bg

[6] Technical University Hamburg-Harburg
Hamburg, GERMANY
email: rohlingr@tu-harburg.de

[7] University of Twente
Enschede, THE NETHERLANDS
email: m.j.bentum@utwente.nl

[8]INESC-ID, Lisboa, Portugal
e-mail: Jorge.fernandes@inesc-id.pt

***Abstract**: Two detection algorithms (heuristic and CFAR) for target detection in pulsar FSR are analyzed using the simulation approach. The simulation results are verified by processing of the experimental data obtained by the radio observatory Dwingeloo in the Netherlands. The simulation and experimental results proved that the CFAR detection algorithm is more effective than the heuristic algorithm and can be successfully used in a pulsar FSR system for protection of air space from unwanted air objects.*

1. Introduction

Pulsar-based Forward Scatter Radar (Pulsar FSR) is a special type of FSR where the pulsar acts as a source of electromagnetic radiation and the radio telescope acts as a receiver. [1.2]. Pulsars

are neutron stars that periodically emit broadband pulses in radio range. In pulsar FSR, the air object can be detected when it crosses a narrow area near the baseline between a pulsar and a radio telescope (the angular deviation from the baseline should not exceed $\pm 5^0$). The possibility to use pulsars as transmitters in pulsar FSR for detection of asteroids is examined in [1] where the power budget of pulsar FSR that can be used for protection of the Earth from unwanted cosmic objects is estimated. The possibility of airplanes detection in a pulsar FSR net is considered in [2].

The main limitation towards designing of detection algorithms is the very low input signal -to-noise ratio (SNR) of the received signals (between -40dB and -90dB) [3]. In pulsar FSR, the processing algorithm for target detection that can be implemented in a radio telecsope includes the following basic stages: (i) - separation of the signal scattered by the target from the direct pulsar signal; (ii) – quadrature detection of the signal from the target; (iii) - non-coherent integration of the received pulses from the target over a large number of repetition periods; (iv) - matched filtering with the filter impulse response according to a given pulsar template and (v) - adaptive signal detection [4,5,6].

The aim of this study is to compare two algorithms for signal detection that can be used in a pulsar FSR system for protection of some air space from unwanted objects. The first approach is to apply the detection algorithm similar to that used in a GPS receiver for automatic acquisition of signals from satellites. This detection algorithm is based on the criterion: the first power peak value should be at least twice the second largest power peak (heuristic approach) [7,8]. The other approach is based on the criterion of Neyman - Pearson, which is very often used for radar signal detection on the background of unknown power (CFAR approach) [9]. The criterion of effectiveness used for comparison of the two detection algorithms is based on their probability characteristics (detection and false alarm). The simulation results are verified by the processing of the experimental data of pulsar B0329+54 recorded in the radio observatory Dwingeloo, the Netherlands.

2. Signal Model

We assume that in FSR, the pulsar pulse sequence re-radiated by the target does not change the pulse form and the repetition period. The simple model of the received target signal can be expressed as a sum of the periodic signal scattered by the target and the receiver noise, which is bandlimited zero mean Gaussian noise of the receiver:

$$y(t) = s(t) + N(0, \sigma^2) \tag{1}$$

The periodic signal from a target can be simulated as convolution between the pulsar pulse shape function (pulse profiles) *p(t)* and the Shah function [4]:

$$s(t) = p(t)\cos(2\pi f_0 t) * \sum_{k=-\infty}^{\infty} \delta(t - kT) \tag{2}$$

Where f_0 is the central frequency and T is the repetition period of pulsar pulses. The pulse profiles of most pulsars presented in the European Pulsar Network (EPN) give grounds to express the function *p(t)* as a sum of several Gaussian pulses [10]. For example, the pulse profile of pulsar B0329+54 can be written as a sum of three Gaussiam pulses:

$$p(t) = \sum_{i=1}^{3} A_i \exp(-\frac{(t - t_i)^2}{2a_i^2} \tag{3}$$

In (3), *Ai* is the maximum of the *i*-th Gaussian pulse at time $t=t_i$, and a_i is a half of the *i*-th Gaussian pulse duration determined at the level of (*Ai*exp(-1/2)).* For pulsar B0329+54 these parameters are:

A_1=16.55; A_2=100; A_3=32.5; t_1=0.2805; t_2=0.30325; t_3=0.3222; a_1=a_2=a_3=0.003.

The real pulse profile of pulsar B0329+54 taken from the EPN and its Gaussian approximation are plotted in Fig.1. The spectrum of the real pulse profile of B0329+54 and the spectrum of the approximated pulse profile are plotted in Fig.2. It can be seen that both the real pulse profile and the approximated pulse profile have the same frequency band, which is about 400 Hz.

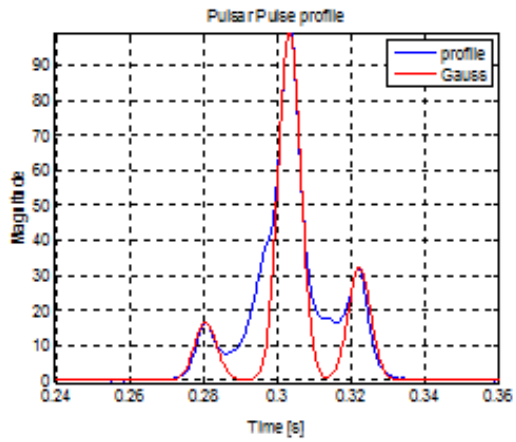

Fig.1 Real and Gaussian pulse profile

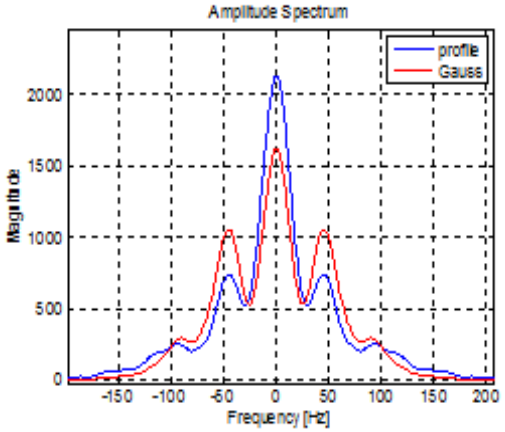

Fig.2: Spectrum of real and Gaussian pulses

The approximated pulse profile allows us to economize the computing system memory of a pulsar-based FSR system. For example, in the computing system memory can be stored only 8 parameters of the pulse profile for B0329+54: 7 parameters for 3 Gaussian pulses and the period of repetition.

3. Signal Processing

The functional block-scheme of the studied signal processing used for target detection in pulsar FSR is shown in Fig.3

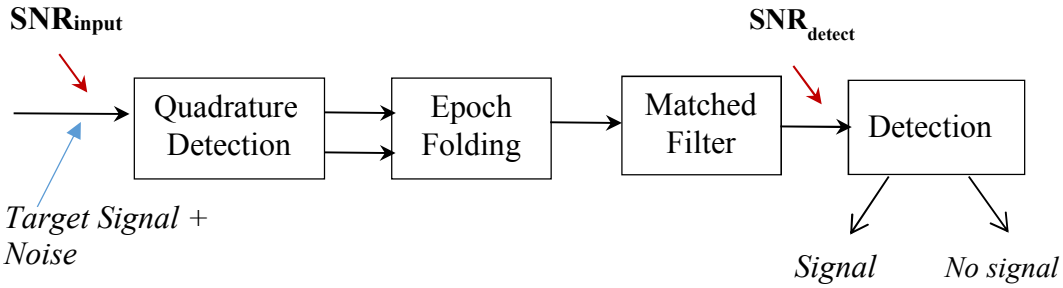

Fig.3: The studied signal processing

The received signal is a mixture of the pulses scatterd by the target and an additive white zero mean Gaussian noise of the receiver (AWGN), whose power is σ^2. After quadrature detection and sampling, the received signal inside one repetition period can be mathematically written in the complex form as:

$$y[nT_s] = I_y[nT_s] + jQ_y[nT_s] \quad (4)$$

In (4), $y[nT_s]$ is the sampled received signal, $I_y[nT_s]$ and $Q_y[nT_s]$ are the sampled quadrature components of the received signal and T_s is the period of sampling. According to [3], the input signal-to-noise ration (SNR_{input}) of the received target signal can be expressed as:

$$SNR_{input} = \frac{S_{ave} A_{eff}}{2k_b T_{sys}} \cdot \frac{\sigma_{FSR}}{4\pi R_{tg}^2} \tag{5}$$

Where k_b is the Boltzman constant (k_b=1.38x10^{-23}WHz^{-1}K^{-1}), S_{ave} is the average pulsar flux density in units of WHz^{-1}m^{-2}, A_{eff} is the effective area of antenna aperture in units of m^2 , T_{sys} is the system Kelvin temperature,σ_{FSR} is the target RCS in FSR, and R_{tg} is the distance to the target.

Epoch folding

If the repetition period T of a pulsar is known, then the input SNR in (5) can be sufficiently improved using the *epoch folding* procedure [3,5]. The input data is broken into a sequence intervals corresponding to the repetition period of the pulsar and then added. When the number of integrated periods grows, the output SNR reinforces with each integrated period. The standard way implemented in most of radio observatories is to integrate the power of the input signal during K sequential periods. In result of epoch folding, the output signal y at time discrete n is formed as:

$$y_{fold}[nT_s, K] = \frac{1}{K}\sum_{k=1}^{K}(I_y^2[nT_s, k] + Q_y^2[nT_s, k]) \tag{6}$$

Where I_y and Q_y are the quadrature components of the input signal y in the time period k. According to [3], after epoch folding, the SNR can be calculated as:

$$SNR_{fold} = SNR_{input}\sqrt{K} \tag{7}$$

Mathced filter

The use of the matched filtering can additionally improve SNR of the target signal before detection. The impulse response of the matched filter is formed as the normalized pulsar power profile [6]:

$$h[nT_s] = p[T_s(N-n+1)] / \left\| p[T_s(N-n+1)] \right\| \tag{8}$$

where $p(nT_s)$ is the sampled pulsar power profile, and N is the filter length.
The performance of the matched filter in the frequency domain can be expressed mathematically as:

$$y_{matched}[nT_s] = IFFT\{H(f) \cdot Y_{fold}(f)\} \tag{9}$$

Where $H(f)$ is frequency response of the matched filter and $Y_{fold}(f)$ is the signal spectrum after epoch folding. As known, the pulsar power profile is different for each pulsar. For example, the power profile of pulsar B0329+54 with the repetition period of 0.7145 s can be simulated using the approximated puse profile shown in Fig.1

The SNR at the matched filter output can be calculated by:

$$SNR_{detect} = SNR_{input} \cdot \sqrt{K} \cdot G_{SP} \tag{10}$$

where G_{SP} is the processing gain of the matched filter.

Heuristic detection algorithm

Similar to the heuristic detection criterion used in GPS for C/A code acquisition in [8], the following algorithm can be used for testing a simple hypothesis H_1 (target signal is present) against a simple alternative H_0 (target signal is absent):

$$\begin{aligned} H_1: &\quad if\ L_{\max,2}\{y_{matched}[nT_s]\} < 0.5L_{\max,1}\{y_{matched}[nT_s]\} \\ H_0: &\quad if\ L_{\max,2}\{y_{matched}[nT_s]\} \geq 0.5L_{\max,1}\{y_{matched}[nT_s]\} \end{aligned} \tag{11}$$

In the decision rule (11), $L_{max,1}$ and $L_{max,2}$ are respectively the first (global) maximum and the second (local) maximum of the signal power $y_{matched}[nT_s]$ (Fig.4). The second maximum $L_{max,2}$ should be searched outside of the target zone that is located around the position of the global maximum $L_{max,1}$. The size of the target zone is determined using the pulsar power profile.

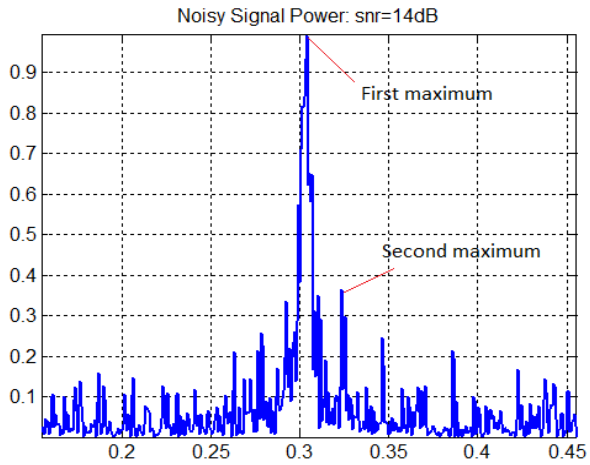

Fig.4 GPS detection approach

CFAR detection algorithm

This approach is based on the Nyman – Pearson criterion, according to which, the following algorithm can be used for testing a simple hypothesis H_1 (target signal is present) against a simple alternative H_0 (target signal is absent) [9]:

$$\begin{aligned} &H_1: if\ \max\{y_{matched}[nT\ ]\} \geq T_{fa}\sum_{l=1}^{L} y'_{matched}[lT_s] \\ &H_0: otherwise \end{aligned} \tag{12}$$

where $y'_{matched}[l,T_s]$ are the signal samples taken from the noise zone. In order to determine the noise zone all signal samples (N) are sorted in the ascending order. The first L samples of so-ordered signal samples form the noise zone $\{y'_{matched}[lT_s]\}$ where l varies in the interval from 1 to L, and L is the noise zone length. In that case the detection constant T_{fa} is determined in accordance with the probability of false alarm, which should be maintained by the detection algorithm. According to the decision rule (12), we assume that the hypothesis H_1 is verified only in one single signal sample. Using the search strategy "Maximum" the probability of false alarm is defined as:

$$P_{FA} = 1 - \left[1 - P_{fa}\right]^N \tag{13}$$

In (13), N is the total number of signal samples of $y_{matched}$, and P_{fa} is the probability of false alarm in a single signal sample. In case of mean zero Gaussian noise, the probability of false alarm to be maintained in a single signal sample is:

$$P_{fa} = 1/(1+T_{fa})^{L} \tag{14}$$

The probability of false alarm in a single signal sample P_{fa} is defined as a solution of the equation (13) for a given probability of false alarm P_{FA}. The solution of the equation (14) gives the detection constant:

$$T_{fa} = P_{fa}^{-1/L} - 1 \tag{15}$$

4. Simulation Algorithm

The Monte Carlo simulation approach for calculation of probability characteristics of the two detection algorithms (heuristic and CFAR) is presented in Fig. 5 – for calculation of the probability of detection and in Fig. 6 – for calculation of the false alarm probability. The probability characteristics of the two detection algorithms (GPS approach and CFAR approach) are calculated using the same simulated data. In order to reduce the simulation time, the input signal and noise are simulated at the output of the matched filter (Fig.3). The noise power is calculated as:

$$\sigma^2 = P_{\max} / SNR_{\det ect} \tag{16}$$

In (16), P_{max} is the maximal amplitude of the target signal (is coosen to be equal to unity). The pulsar power profile for B0329+54 needed for the matched filtering is obtained using the approximated pulse profile (Fig.1) as $p^2(t)$.

The probability characteristics are calculated for a set of values of SNR_{detect} in range from 0 dB to 30 dB with a step of 2 dB. In order to obtain the high level of confidence, the number of Monte Carlo runs is chosen to be N_{sim}=10000.

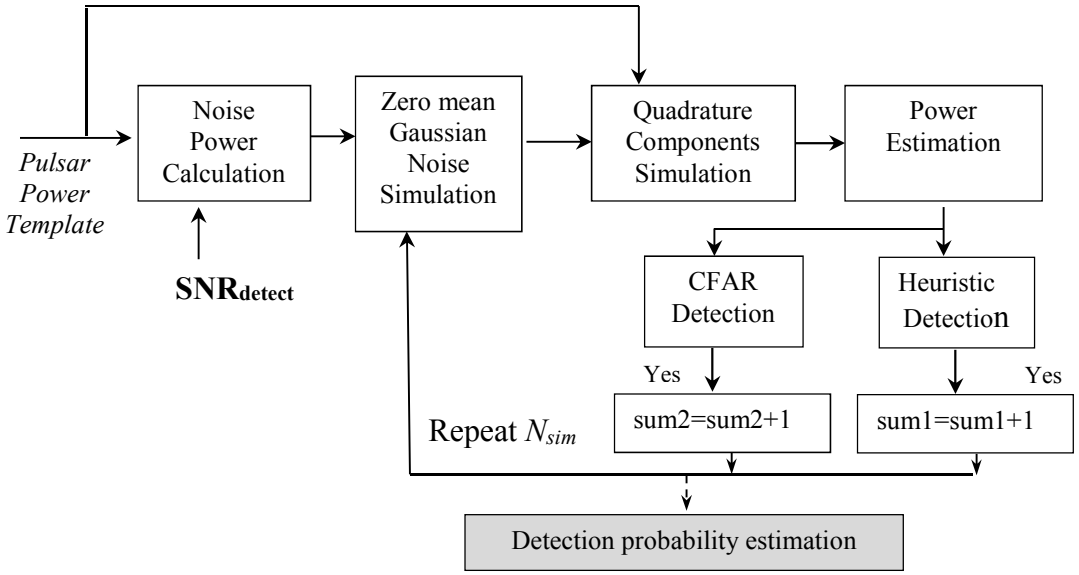

Fig.5 Simulation algorithm for calculation of the detection probability

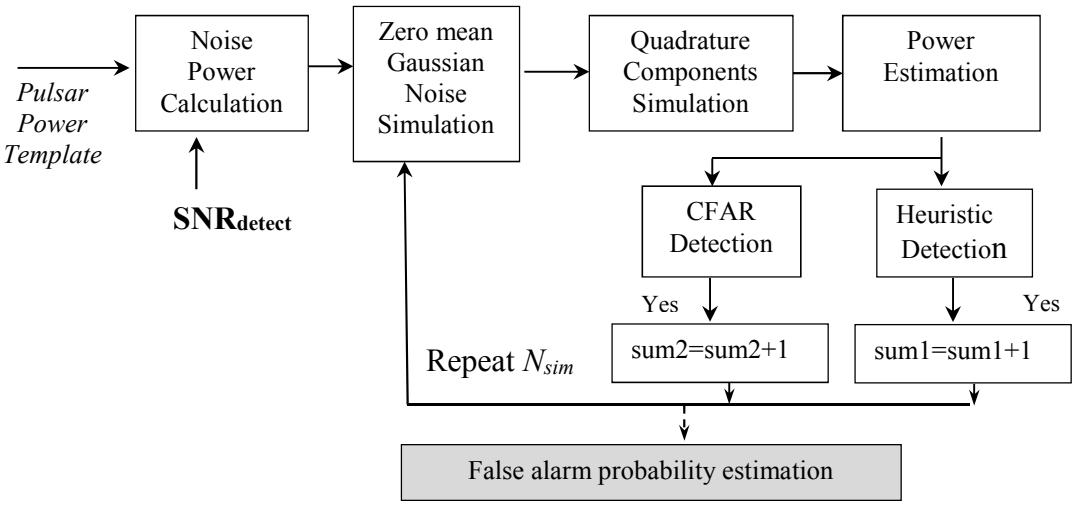

Fig.6 Simulation algorithm for calculation of the probability of false alarm

5. Simulation Results

The effectiveness of the two detectors (heuristic and CFAR) is expressed in terms of their probability characteristics (detection probability and false alarm probability), which are calculated using the Monte Carlo approach. The simulated CFAR detector is designed to maintain the false alarm probability of 0.01. It should be noted that the two detection algorithms use the same noise zone for their operation. The two calculated probability characteristics are plotted depending on the input SNR of the detector (SNR_{detect}). The detection probabilities of the two detectors are plotted in Fig.7, and the false alarm probabilities are plotted in Fig.8.

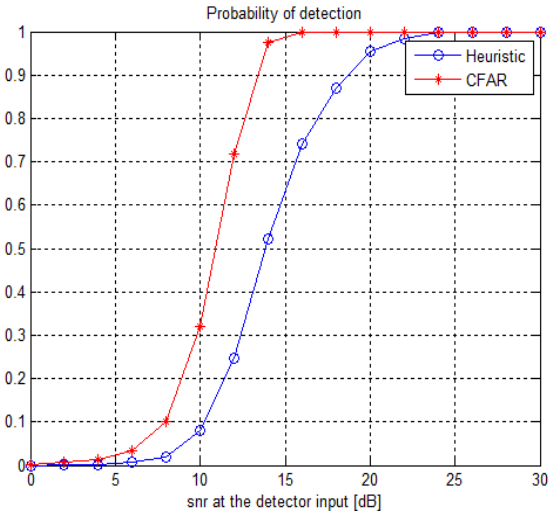

Fig.7 Estimated detection probability

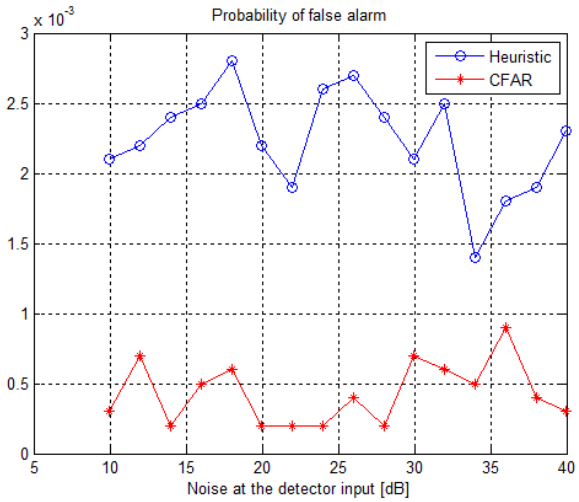

Fig.8 Estimated false alarm probability

The probability characteristics presented in Fig.7 and Fig.8 show that the CFAR algorithm guarantees the greater efficiency than the heuristic detector. It means that the CFAR detector allows obtaining the higher probability of detection at the lower probability of false alarm than the heuristic detector.

6. Experimental Results

The effectiveness of the same two detectors, mentioned above, is verified by processing of the experimental data of pulsar B0329+54 provided by the radio observatory Dwingeloo, the Netherlands. The processing of the experimental data includes the same basic stages, described in Section 2: epoch folding of the data over a set of periods; calculation of the impulse response of the matched filter; matched filtering in the frequency domain; heuristic/CFAR signal detection. The observing frequency is 1330 MHz, which corresponds to the frequency of 21.4 MHz in the recorded IF-data. The total bandwidth recorded is about 30 MHz, 15 MHz to each side of this 21.4 MHz central frequency. The input 10-bit signal is sampled at the frequency of 70 MHz. The output signal of the epoch folding is sampled at frequency of 70 MHz, and the matched filter is applied after the epoch folding algorithm.

In result of processing, the output signals of the matched filter with the corresponding detection thresholds of the two detectors (heuristic and CFAR) are given in Fig. 9 and Fig.10, for 250 and 400 integrated periods. From Fig.9 for 200 integrated periods can be seen that the threshold of the CFAR detection is lower than that of the heuristic detector. It means that in that case the detection probability of the CFAR detector is higher than that of the heuristic detector. When the number of integrated periods grows to 400 the thresholds of both detectors become nearly the same. It means that when the number of integrated period is very large, the SNR at the matched filter output is also very high and the probabilities of detection of both detectors are nearly the same. It can be seen that the results, obtained by the processing of the experimental data in this Section, support the results, obtained by simulation in previous Section, i.e. the CFAR detector is more effective than the heuristic detector.

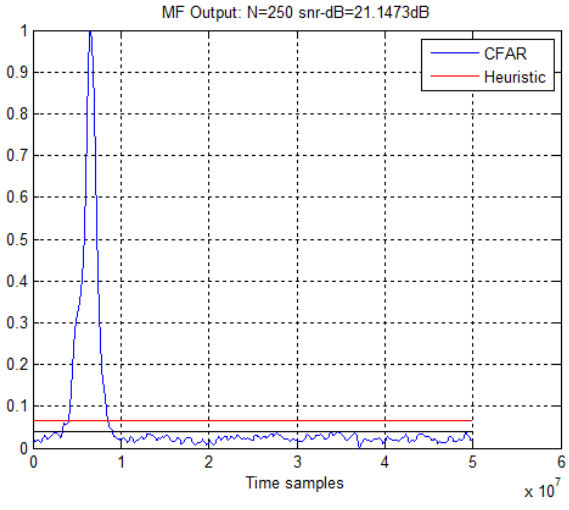

Fig.9 Matched filter output (N=250)

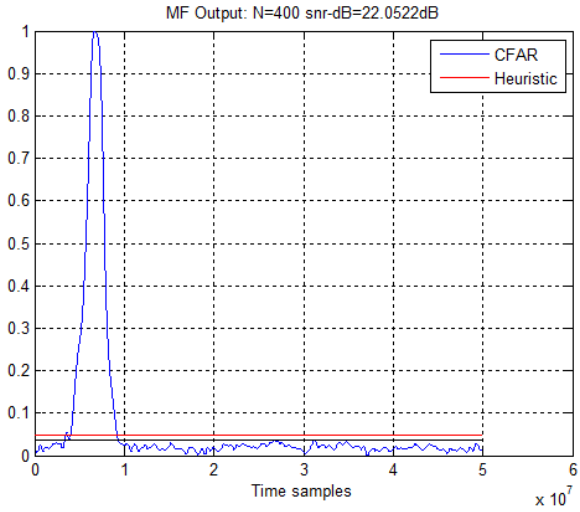

Fig.10 Matched filter output (N=400)

Acknowledgment

This work is partly supported by the project DN 07/1/14.12.2016

References

[1] C. Kabakchiev C., V. Behar, I. Garvanov, D. Kabakchieva, A. Kabakchiev, H. Rohling, M. Bentum, J. Fernandes, „Feasibility of asteroid detection using pulsar signals", International conference on radar systems, 23 – 26 October 2017, Belfast Waterfront Conference Centre, UK.

[2] Kabakchiev C., V. Behar, I. Garvanov, D. Kabakchieva, A. Kabakchiev, H. Rohling, M. Bentum, J.Fernandes, "Feasibility of Air Target Detection using Pulsar FSR Net", European Radar Conference 2017, 11th – 13th October 2017, Nuremberg, Germany.

[3] X. D. Lorimer and M. Kramer, Handbook of pulsar astronomy, Cambridge university press, N.Y.,2005.

[4] J. Sala et al., Feasibility study for a spacecraft navigation system relying on pulsar timing information, Tech. Rep. 03/4202, ARIADNA Study, June 2004.

[5] P. Buist, S. Engelen, A. Noroozi,, P. Sundaramoorthy, S. Verhagen and C. Verhoeven, "Overview of Pulsar Navigation: Past, Present and Future Trends", *Journal of the Institute of Navigation*, 2011, vol.58, no 2, pp. 153-164.

[6] R. Heusdens, S. Engelen, P. Buist, A. Noroozi, P. Sundaramoorthy, C. Verhoeven, M. Bentum and E. Gill, "Match Filtering Approach for Signal Acquisition in Radio-Pulsar Navigation", *Proc. of the 63rd International Astronautical Congress*, Naples, Italy, 2012, IAC-12-B2.6.10

[7] J. Bao-Yen Tsui, Fundamentals of Global Positioning System Receivers: A Software Approach, Wiley Interscience, John Wiley & Sons, 2005.

[8] K. Borre, D. Akos, N. Bertelsen, P. Rinder and S. Jensen, A software-defined GPS and Galileo receiver: A single frequency approach, Birkhäuser, Boston, 2007.

[9] H.M. Finn, H. M. and R.S. Johnson, "Adaptive detection mode with threshold control as a function of spatially sampled clutter estimation", *RCA Review*, 1968, vol. 29, no 3, pp. 414-464

[10] The EPN pulsar database**,** available in http://www.naic.edu/~pulsar/data/browser.html